Program Digest, 2019 IEEE International Ultrasonics Symposium (IUS)
Glasgow, Scotland, October 6-9, 2019

A Single Ultrasonic Transducer Fast and Robust Short-Range Distance Measurement Method

Daniel Lagler*, Sebastian Anzinger†, Eugen Pfann*, Alessandra Fusco‡, Christian Bretthauer‡ and Mario Huemer*
*Institute of Signal Processing, Johannes Kepler University Linz, Austria
†Department of Microsystems Engineering, Albert Ludwig University of Freiburg, Germany
‡Infineon Technologies AG, Neubiberg, Germany

***Abstract*—Capacitive micromachined ultrasonic transducers (CMUTs) enable the design of small and low-cost proximity sensors for application areas such as embedded systems. Precise short-range distance measurements are achieved via time-of-flight (TOF) estimation based on the transmission of frequency modulated signals and pulse compression on the received echo. In single CMUT transceiver designs, the lower limit of the detection range is constrained by the transmit pulse width and membrane ringing, resulting in a blanking zone where no echo signal can be detected. This contribution describes a low complexity method based on customized transmit pulses and partial ringing removal to reduce the minimum detectable range down to 3 cm, while maintaining high precision at larger distances of up to 30 cm.**

***Index Terms*—distance measurement, time of arrival, ultrasonic transducers, matched filters, pulse compression, ringing**

I. Introduction

Ultrasonic ranging enables numerous applications in the fields of localization, positioning, navigation and robotics. It can be used in all types of media such as gases, fluids and solid bodies. The advantage of airborne ultrasound lies within the low complexity, durability and small size of its systems, which allows for cost-effective solutions and the potential use in embedded devices.

The most common approach for ultrasonic ranging is the estimation of the time-of-arrival (TOA) or time-of-flight (TOF) [1] and subsequent calculation of the distance using measurements or estimates of the speed of sound. This method is also applied in echo-based ranging, which estimates the distance between an ultrasonic transceiver and an arbitrary object acting as acoustic reflector. Alternative approaches are either based on measuring the direction-of-arrival (DOA) [2], also referred to as angle-of-arrival (AOA), at several receivers, followed by multiangulation, the received signal strength (RSS) or by estimating the phase-of-arrival (POA) of multiple frequency components [3].

The easiest way to determine the TOF is by thresholding and subsequent maximum search in the received signal or direct detection of the beginning of the pulse. On the other hand, cross-correlation and related methods optimize the signal-to-noise ratio (SNR) with a priori knowledge of the expected echo before estimating the TOF. In analogy, cross spectrum techniques try to achieve the same in the frequency domain.

When considering echo-based ranging with single CMUT transceivers, the smallest detectable distance is limited by the blanking zone [4], where no echo signal can be evaluated. The duration of the blanking zone is defined by the chosen transmit pulse width and the transducer membrane ringing. For short-range distance measurements, it is essential to reduce the ringing via transmit pulse [5] and receive filter [6] optimizations.

This contribution proposes a single transducer short-range distance measurement method for fast and robust ranging between 3 and 30 cm. The technique takes into account prior knowledge of manufacturing tolerances of the transducers and assumes that calibration of every single device is not possible, which makes it potentially attractive for mass market applications.

II. Transducers

The design and properties of the investigated short-range distance measurement system builds on the characteristics of the capacitive micromachined ultrasonic transducers (CMUTs), fabricated in dual-backplate technology by Infineon Technologies AG (see Fig. 1) [7].

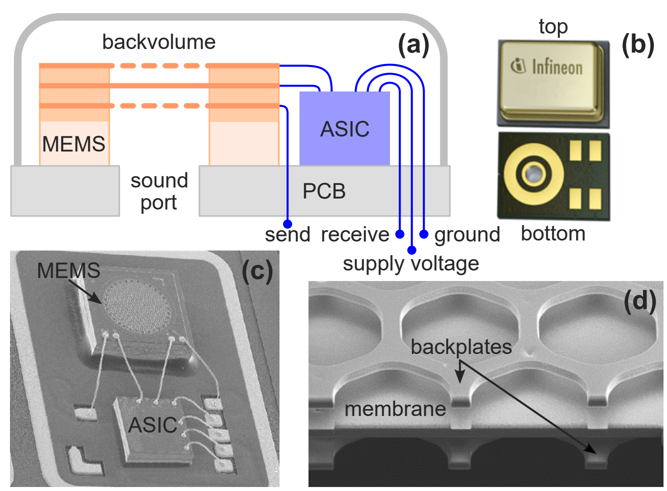

Fig. 1. (a) Schematic of the transducer module consisting of a MEMS, ASIC, PCB and metallic lid, (b) ultrasonic transceiver package, (c) SEM picture of an assembled prototype and (d) zoomed view of the membrane and backplates.

The microelectromechanical system (MEMS) transducers consist of a circular poly-silicon membrane with a thickness of a few hundred nanometers placed between two highly

978-1-7281-4595-2/19/$31.00 ©2019 IEEE

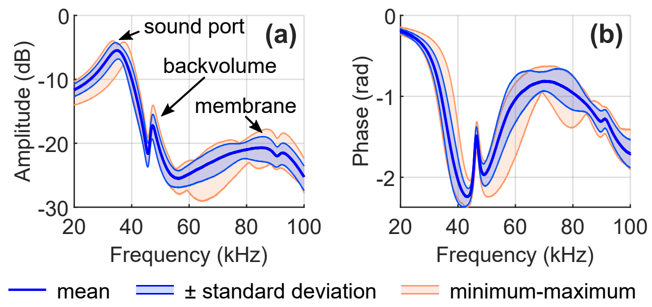

Fig. 2. (a) Amplitude and (b) phase response with manufacturing tolerances including mean, ±standard deviation and minimum to maximum range determined by 10 transducer samples.

perforated counter electrodes (backplates) forming a capacitive system. Compared to classical CMUTs, consisting of a membrane placed upon an evacuated cavity [8], the transducers under test have a ventilated cavity, resulting in an increased bandwidth around the resonance frequencies as viscous damping is introduced into the capacitive system. Additionally, ventilation holes are added to the membrane, making the transducer insensitive to static pressure changes.

A transceiver functionality is enabled by connecting the membrane and the top backplate to an application-specific integrated circuit (ASIC), supplying the membrane with a tunable bias voltage and allowing a broadband readout in the audio and ultrasonic frequency range. By applying an electrical actuation pattern to the remaining backplate, a corresponding attractive electrical force is generated, which actively brings the membrane into an oscillation, hence radiating ultrasonic waves. Consequently, the sending and receiving circuitry remain separated, resulting in an increased device SNR as no electrical switches introducing additional noise are required.

A schematic of a full CMUT module is depicted in Fig. 1a and a scanning electron microscope (SEM) image of an assembled prototype in Fig. 1c. The MEMS and ASIC are both placed on a printed circuit board (PCB) containing a sound inlet, called sound port. To protect the sensitive MEMS, a metallic lid is soldered on the PCB, resulting in a full module size of $4 \times 3 \times 1\,\mathrm{mm}^3$. A detailed description of the transducer characteristics, including generated sound pressure levels and receiving sensitivity, are discussed in [7]. With an ASIC supply voltage of $3\,\mathrm{V}_{\mathrm{DC}}$ and an always on power consumption of the readout electronics of $350\,\mu\mathrm{W}$, the sensor allows for an integration into space and power critical systems.

The ultrasonic part of the transducer frequency response with manufacturing tolerances is presented in Fig. 2. The MEMS and its interaction with the transducer package lead to multiple resonance peaks. The 36 kHz peak originates from an acoustic Helmholtz resonance of the sound port, and the 90 kHz resonance is the mechanical resonance of the MEMS membrane. Details about a physical description and modeling of the system are described in [7].

III. Proposed Method

The proposed method for measuring short-range distances with single ultrasonic transceivers is outlined in Fig. 3.

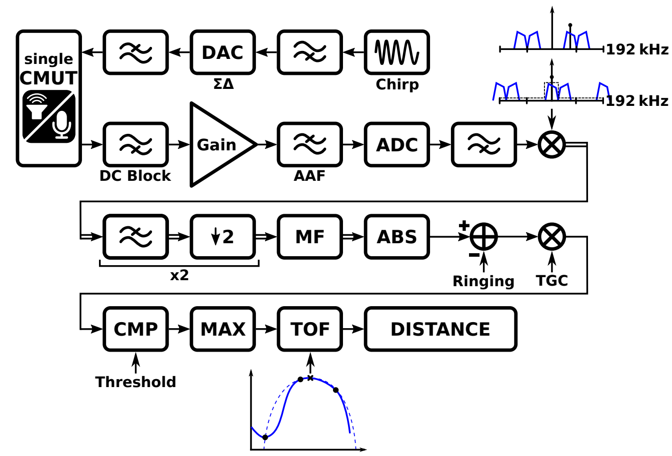

Fig. 3. Overview of the proposed short-range distance measurement method including a single CMUT transceiver, transmit (Tx) and receive (Rx) processing pipelines.

The upper part of Fig. 3 shows the Tx processing pipeline. To generate the actuation signal for the ultrasound transducer, a down-chirp ranging from 80 to 65 kHz is filtered with a 5[th] order infinite impulse response (IIR) high-pass filter with Cauer characteristics and 65 kHz cutoff frequency. The purpose of the high-pass filter is to suppress frequency components in the transmit pulse corresponding to the transducer resonances at around 36 kHz and 50 kHz (see Fig. 2). Although, high-pass filtering increases the total duration of the transmit pulse, Fig. 4 shows that due to reduced ringing excitation the resulting receive pulse duration is shortened. Additionally, high-pass filtering concentrates the transmit power at high frequencies where the transducer exhibits a flatter frequency response (see Fig. 2). Finally, sigma-delta modulation digital to analog conversion (DAC) can be used followed by a low-complex analog low-pass filter to achieve reduced hardware complexity.

The lower part of Fig. 3 gives an overview of the Rx processing path. After removing the direct current (DC) component, the received signal is amplified for the optimal usage with a low-cost ADC's dynamic range. A conventional analog anti-aliasing filter (AAF) is applied before ADC conversion which occurs at the audio sampling frequency of 192 kHz.

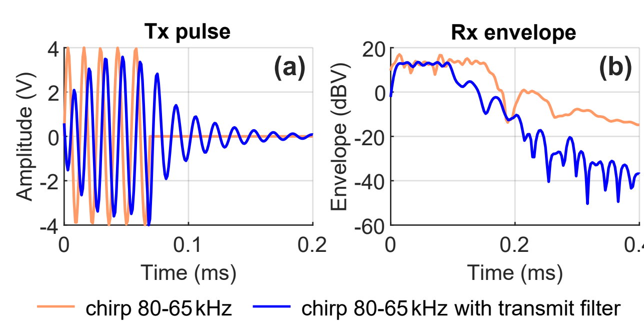

Fig. 4. (a) Transmit pulse shape with/without Cauer high-pass filter and the (b) associated received signal envelopes showing the ringing in absence of echos.

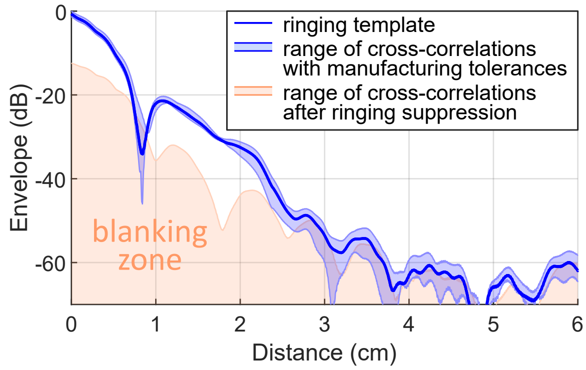

Fig. 5. Ringing template generation considering manufacturing tolerances, ringing suppression by template subtraction and improved blanking zone after ringing reduction.

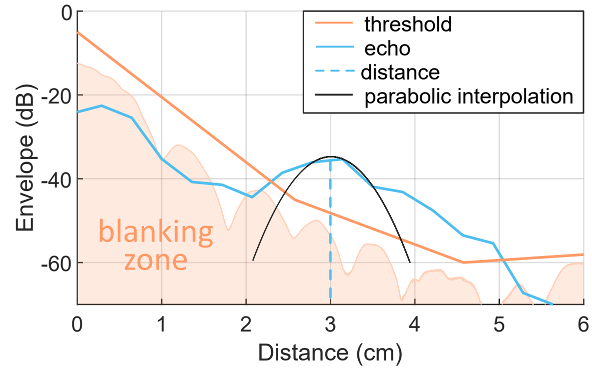

Fig. 6. Cross-correlation envelope with echo at 3 cm, maximum deviations of several transducer samples without echo, linearized threshold and parabolic interpolation.

The digital signal is filtered with a low-complex 3rd order Cauer high-pass IIR filter with a cutoff below 60 kHz to remove audio and lower ultrasonic frequencies. As indicated in Fig. 3, quadrature demodulation shifts the frequency band between 48 to 96 kHz to around DC to generate the complex baseband signal with a bandwidth of 24 kHz [9]. Two stage decimation is used to reduce the sampling rate to 48 kHz with an intermediate step at 96 kHz using low-complexity 3rd order Cauer halfband decimation filters in either stage.

A matched filter (MF) is used to obtain the cross-correlation between the received signal and the complex conjugate of the estimated echo pulse. This leads to pulse compression and optimizes the SNR provided that a sufficient accurate echo estimate is available and assuming an additive white Gaussian noise (AWGN) channel [6]. To account for different gains in individual transducer samples, the cross-correlation sequence maximum is normalized. Computational complexity can be further reduced by omitting the square root and performing subsequent operations on the absolute squared signal values.

A low-complexity approach for ringing suppression is the use of ringing look-up-tables where subtraction of a ringing template is either performed on complex IQ data or on the corresponding magnitude. The latter approach is preferable since no accurate phase alignment between the template and the cross-correlation time series is required. As shown in Fig. 5 the ringing template is obtained by an average of the cross-correlations between transmit signal and receive signals without any echo over a range of transducer samples in order to consider manufacturing tolerances. Without ringing suppression the blanking zone is given by the maximum of the cross-correlation range as illustrated in Fig. 5, considering the transducer manufacturing tolerances. After subtraction of the ringing template a reduced blanking zone is obtained, which is now given by the maximum difference between the ringing curves of any individual transducer and the ringing template. The blanking zone is used to define a threshold which must be exceeded by echos to be detectable.

Alternative, more complex approaches to deal with transducer tolerances in ringing reduction were reported in the literature, for example using a template library [10]. Nevertheless, these approaches tend to be too complex for many embedded solutions.

An approximate time gain compensation (TGC) via multiplication by distance or alternatively by a precomputed TGC look-up table is applied to normalize the cross-correlation envelope values by balancing out the loss in energy of ultrasonic waves with distance. Finally, the TOF is obtained by the point in time where the cross-correlation envelope displays its maximum and which is above the threshold. Additionally, the measurement resolution can be enhanced via parabolic interpolation.

The time-dependent threshold is calculated by the upper bound of several measurements of multiple transducer samples plus a small extra increment proportional to the quantization noise. A piecewise linear spline approximation of the threshold reduces the storage requirements, only on the expense of a per-sample linear interpolation. In particular, in the range where ringing effects are negligible the threshold can be approximated by a single line element. Fig. 6 outlines the described TOF based distance estimation method using a piecewise linear threshold and an acoustic reflector placed at 3 cm distance from the transducer. TGC was omitted in Fig. 6 to allow a comparison with Fig. 5.

IV. Results and Discussion

Measurements are performed with an experimental setup consisting of a CMUT transceiver, a low-complex analog circuit and a combined programmable signal generator and oscilloscope device. Transmit pulses are sent and echos received using a Matlab script controlling the measurement device via a C++ software interface. The transmit pulses are amplified to 8 V_{PP} in order to obtain an echo peak SNR of 12 dB at 30 cm distance. A large size planar reflector with a hard surface for good reflection properties is placed in front of the transducer, orthogonal to the transducer axis.

A. Precision

The precision of the proposed short-range distance measurement method is evaluated by calculating the standard deviation

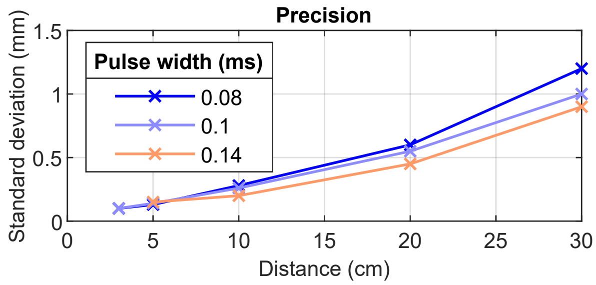

Fig. 7. Measured precision by calculating the standard deviation of 200 measurements with 3 different pulse widths of 0.08, 0.1 and 0.14 ms, which are measured at 50 % of maximum amplitude.

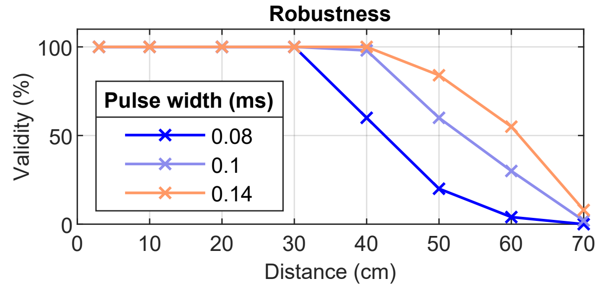

Fig. 8. Robustness value comparison of generated Tx signals with 3 different pulse widths of 0.08, 0.1 and 0.14 ms, which are measured at 50 % of maximum amplitude.

of 200 measurements averaged over 6 transducers at distances of 3, 5, 10, 20 and 30 cm (see Fig. 7). The precision of transmit pulses with different pulse widths is presented.

B. Computational Complexity

The received signal is acquired with a sampling rate of 192 kHz, resulting in a minimum of 400 samples to cover a range of 30 cm. Precomputation of the complex exponential terms reduces the demodulation to a component-wise multiplication of the signal by a constant vector of sines and cosines. All Cauer IIR filters in the design are implemented as cascaded second order structures and can be optimized in hardware by reducing the number of shift-and-add operations in multipliers [11]. The 48 kHz demodulated Rx signal with 100 samples is filtered by a 15-tap matched filter, leading to 86 complex cross-correlation samples. Table I shows a per-step comparison of the required number of real-valued multiplications and additions between the proposed method decimating to a sampling rate of 48 kHz and a reference system which performs all operations at the original sampling rate of 192 kHz.

TABLE I
ESTIMATED COMPLEXITY

	Low-complex		**Reference**	
Step	MUL	ADD	MUL	ADD
High-pass filter	3200	2400	3200	2400
Demodulation	800	-	-	-
Decimation	4800	3600	-	-
Matched filter	5160	3784	20460	20119
Envelope	172	86	1364	341
Ringing reduction	-	10	-	40
Time gain compensation	86	-	341	-
Thresholding	-	86	-	341
Maximum	-	85	-	340
Sum	14218	10051	25365	23581

C. Robustness

The robustness of the method is investigated by checking the validity of several measurements on six transducer samples. A robustness of 90 % is obtained if 90 out of 100 measurements are valid. A TOF is valid, if the cross-correlation envelope peak lies above the threshold and if it is close to the expected TOF. Fig. 8 shows the robustness of the algorithm evaluated at distances of 3 to 70 cm.

V. Conclusion

The methodology described in this contribution proved to be an effective and low-cost short-range distance measurement approach for resource limited applications such as embedded systems. Depending on the specific application, hardware limitation and desired accuracy, algorithm parameters, e.g. the demodulation frequency bandwidth, can be tuned in order to meet the expectations. The method facilitates large-scale applications since no explicit calibration of every single device is necessary.

References

[1] J. C. Jackson et al., “Time-of-flight measurement techniques for airborne ultrasonic ranging,” IEEE Trans. Ultrason. Ferroelectr. Freq. Control, vol. 60, no. 2, pp. 343–355, 2013.
[2] D. Caicedo and A. Pandharipande, “Distributed ultrasonic zoned presence sensing system,” IEEE Sens. J., vol. 14, no. 1, pp. 234-243, 2014.
[3] M. M. Saad, C. J. Bleakley, S. Dobson, and S. Member, “Robust high-accuracy ultrasonic range measurement system,” IEEE Trans. Instrum. Meas., vol. 60, no. 10, pp. 3334–3341, 2011.
[4] M. Ramankutty, D. Kumar Kokkoden, S. Prasanna Sudhakaran, B. Chambalon and N. Mathew, “Non contact high precision distance measurement using single probe ultrasonic transducer,” Proc. World Conf. NDT, 2016.
[5] A. Lindo, E. García, J. Ureña, M. Del Carmen Pérez, and Á. Hernández, “Multiband waveform design for an ultrasonic indoor positioning system,” IEEE Sens. J., vol. 15, no. 12, pp. 7190–7199, 2015.
[6] D. Ruiz, E. García, J. Ureña, J. M. Villadangos, J. J. García, and C. De Marziani, “Performance comparison of correlation-based receive filters in an ultrasonic indoor positioning system,” Proc. IEEE Instrum. Meas. Technol. Conf., pp. 1548–1551, 2014.
[7] S. Anzinger, C. Bretthauer, J. Manz and A. Dehé, “Broadband acoustical MEMS transceivers for simultaneous range finding and microphone applications,” Proc. Transducers & Eurosensors XXXIII, pp. 865-868, 2019.
[8] Y. Qiu et al., “Piezoelectric micromachined ultrasound transducer (PMUT) arrays for integrated sensing, actuation and imaging”, IEEE Sens. J., vol. 15, no. 4, pp. 8020-8041, 2015.
[9] L. Angrisani and R. Schiano Lo Moriello, “Estimating ultrasonic time-of-flight through quadrature demodulation,” IEEE Trans. Instrum. Meas., vol. 55, no. 1, pp. 54–62, 2006.
[10] P. S. Subodh, M. Nimmy, R. Murali and C. Byju, “A novel method for reverberation cancellation in single ultrasonic transducer based measurement systems.” Proc. NDE, 2015.
[11] M. D. Lutovac and L. D. Milić, “Design of computationally efficient elliptic IIR filters with a reduced number of shift-and-add operations in multipliers,” IEEE Trans. Signal Process., vol. 45, no. 10, pp. 2422–2430, 1997.